Original Article	*Curr. Appl. Sci.*, **2025**, *3*(1): 47-56 DOI:10.22034/cas.2024.456324.1039	Current Applied Sciences

Effect of Constrained Studded Pressing on the Microstructure and Residual Stresses for Producing Nanostructure Pure Copper Sheet

Mohamad Mahdi Kaykha

Department of Mechanical Engineering, Faculty of Engineering, University of Zabol, Zabol, Iran

Corresponding author's e-mail: *mm.kaykha@uoz.ac.ir*

Article Information

Received: 07 May 2024
Revised: 11 June 2024
Accepted: 11 June 2024
Published online: 02 April 2025

Keywords

Constrained studded pressing
Copper sheet
Microstructure
Residual stress
Severe plastic deformation

Abstract

Severe plastic deformation (SPD) have been established to produce ultrafine-grained and nanostructure materials. One of the newly introduced methods is the constrained studded pressing (CSP) technique. A limitation of the CSP process is the creation of surface cracks. The most essential factors affecting surface cracks are residual stresses. In the current research, residual stresses distribution was studied on copper sheet under CSP using the finite element method. In addition, for laboratory study, microstructure and residual stress evaluation were studied before and after applying the CSP method. The microstructures of the annealed and deformed copper sheets have been observing by an optical microscope. The grain size, dislocation density, and the residual stresses were tested using an X-ray diffraction. The average grain size decreased from 27 μm in the annealed sample to 11 μm in the first pass sample. In the 10th pass, the average grain size decreased to 750 nm. The smallest reduction in grain size was achieved after applying the first pass, but with the increase of the applied strain in the final pass, the highest dislocation density was created in the microstructure. Therefore, by increasing the density of dislocations and followed by dynamic recovery, it caused the largest decrease in grain size compared to other samples. The residual stresses were altered from +153.2 MPa for the annealed sample to -48.6 MPa in the 10th pass sample. According to this research, the application of more strains is directly related to the creation of compressive residual stresses and grain refinement.

1. Introduction

Today, the severe plastic deformation (SPD) methods are increasing dramatically [1]. The most crucial feature of SPD techniques is that, after forming, the dimensions of the sample remain constant. SPD techniques are divided into three categories (according to the geometry): tubes, bulk and sheets materials. The most common sheets are

repetitive corrugation and straightening (RCS) [2] constrained groove pressing (CGP) [3], and constrained studded pressing (CSP) [4]. According to the die geometry in the CSP method, there is no need to rotate the sample after each pass, and each pass includes two pressing steps. The equivalent plastic strain in the CSP is 0.82. On the other hand, the equivalent plastic strain of the CSPed sample is 20.7% higher than the CGPed sample [4]. Among them, most important influential factors in CSP are the friction between dies and sheet, sheet thickness, and the geometric design of the dies [5]. Thangapandian et al. [6] investigated the strain values by applying semicircular geometric profiles dies and CGP for AA5083 aluminum. They reported that in dies with flat groove geometry, cracks occur at low passes due to the sharp edges of the grooves, while in dies with semicircular geometry, cracks are delayed and observed at higher passes. Lee et al. [7] considered the influence of die geometry on the microstructural evaluation of metal sheets through simulation and experiments. They reported that the shear strain on the inclined area while the flat parts remain without plastic deformation. Therefore, in this type of geometric of dies, the problem of non-uniformity of strain is observed. Yoon et al. [8] numerically studied the strain localization in CGP method on copper sheet using Abaqus software. They reported that the inhomogeneous strain distribution and the presence of regions of lower will cause cracks. Similar to Yun and his colleagues, Wang et al. [9] stated that because of the interface area, three-dimensional stresses and stress concentration are created. On the other hand, the deformation in the inclined region is a combination of shear, bending and tensile deformation. Therefore, the distribution of the effective plastic strain is heterogeneous [8, 9]. In 2020, Kumar et al. [10] reported that using the modifications of the profile geometry of CGP, not only increasing the number of deformations passes, but also delayed initiation and cracks growth. Sajadi et al. [11] reported that with the increase of groove angle, the tendency to crack on aluminum sheets by the CGP method increased. The most critical challenges of the CGP techniques are the inhomogeneous distribution of the plastic strain and the formation of microcracks. Therefore, these surface cracks cause the creation of cracks in the early stages of pressing and the lack of complete filling of the die space, especially on the sharp edges [6, 11, 12]. In 2020, Elizalde et al. [13] investigated the effect of the RCS process on the microstructure and mechanical properties of Al-6061 sheets. They used molds with semicircular sinusoidal grooves to reduce stress concentration. The results show a significant increase in the yield strength of the samples with an increase in the number of passes. Also, Shahraki and his colleagues [14] produced ultra-fine grain steel using the CGP pressing method. They showed that the grain size of the samples decreased significantly after applying the CGP process and increased the strength and hardness. Horpisheh and Nazari [15] studied the effect of CGP process on the microstructural and mechanical properties of copper sheets. Their results showed that by using the CGP process, the strength and hardness of the samples increase dramatically. Also, the images prepared with an optical microscope show a decrease in the grain size from 60 micrometers in the annealed sample to 1 micrometer in the sample after three passes of pressing operation. Therefore, so far, most of the studies are on microstructural evaluation and mechanical properties of nanostructures produced by CGP and CSP processes. On the other hand, the effects of the resulting grain refinement in relation to the residual stresses created in the production samples of the production sheet have not been investigated. According to the studies carried out in the process of SPD, the comparison of the residual stresses created in different passes of the CSP process will create a new approach in the research. One of the scientific fields that needs more investigate is the correlation between residual stresses and microstructural evaluation. Therefore, in this research, the relationship between changes in microstructural properties and residual stresses is studied. In this research, the influence of the CSP method on the

microstructure, residual stresses, and mechanical properties of commercially pure copper sheets is investigated numerically and experimentally.

2. Materials and Methods

In this research, commercial pure copper sheets were used. The copper sheet used has a purity of 99.9%. Samples with dimensions of 50mm×50mm×2mm were cut. To eliminate stresses and create a homogeneous structure, the copper sheets were annealed for 2 hours at 650 °C. Hydrochloric acids were used to deoxidize and clean the samples. Forming was performed using a 50-ton hydraulic press with a constant speed of 0.1 mm/s at ambient temperature. Then, samples were prepared for metallographic testing. The process of corrugation and straightening continued up to the 11th pass, which led to the crack initiation of the sheet. An Olympus BH2 optical microscope were used to observe the microstructural evaluations of the sheets. To prepare metallographic samples, samples with dimensions of 2 mm × 2 mm × 1 mm are cut from the middle of the sheet and mounted. After sanding with 200, 400, 800, 1000, 2000, and 2500 sandpapers, the samples were polished with a polishing pad at 200 rpm. Samples were washed with alcohol. Keller's solution with a combination of 20 ml HNO_3, 4 ml HCl, 2 ml HF and 175 ml distilled water was used to etch metallographic samples. X-ray diffraction (XRD) test was used to evaluate the microstructural characteristics of the samples. For this purpose, the XRD PW1730 machine was used to measure grain size and analyze residual stresses. The X-ray diffractometer PW1730, that uses a copper lamp with an accuracy of 0.05 in 2θ and a wavelength of 1.54 Å. X-ray diffractometer analysis is from 10 degrees to 80 degrees. Peak width at half height, angle 2θ was calculated from X-ray diffraction test patterns. Errors due to the instrumental effect of Warren's method were also calculated. Also, the results were used to approximate the amount of the residual stresses from the XRD results. The research steps and sample coding are shown in flowchart of Figure 1 and Table 1.

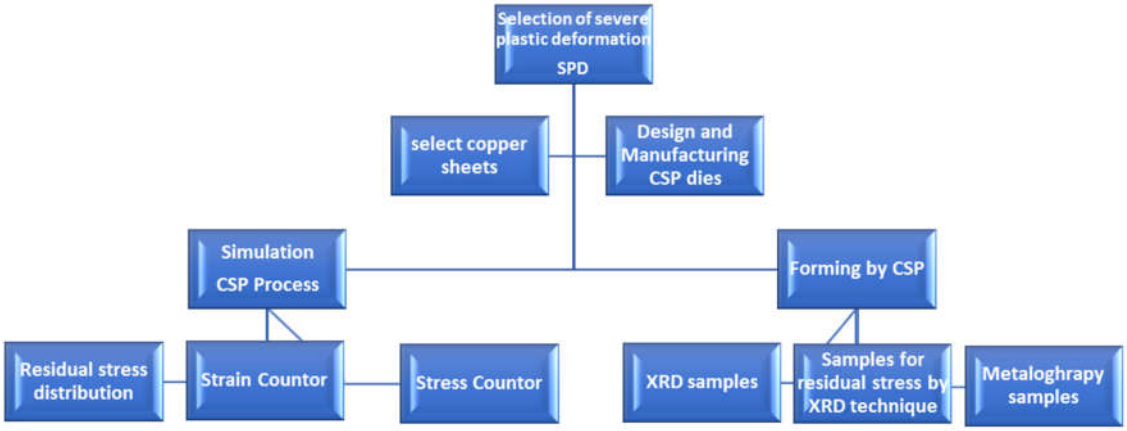

Figure 1. Flowchart of research steps

Table 1. sample coding and number of tests

Test	The purpose of the experiment	number of samples	Pass No.
Metallography	Grain size	3	1,10 and as received
XRD	Grain refinement	3	1,10 and as received
XRD	Residual stresses	3	1,10 and as received

3. Results and Discussion

3.1 *Microstructure*

Figure 2 illustrates the images of annealed sample, first and tenth passes of CSPed copper sheets taken by optical microscope. To measure grain size, Hein's method was used [16]. Consisting with Figure 2-a, the average grain size of the annealed sample is about 27 micrometers. According to Figure 2-b and 2-c, for first and 10th passes, due to the impose of SPD, the grain size has decreased. According to Figure 2-b and 2-c for the first and tenth passes, the size of the grains is greatly reduced. The reason for the drastic reduction in the grain size can be attributed to the implementation of intense strain according to the geometry of the dies.

Due to the sharp decrease in the grain size in the tenth pass, therefore, in order to calculate the grain size created after applying the CSP process, using the information obtained from the XRD patterns (shown in Figure 3) and the Williamson-Hall relation, it was calculated [17]. According to Figure 2-b and 2-c, the average grain sizes in the first pass and the final pass are approximately 11 µm and 750 nm. One of the most important reasons for the sharp decrease in grain size is the increase in the density of dislocations and their movement. An increase in the density of dislocations leads to the formation of subgrain structures. Numerous researchers have similarly reported that grain size changes have an inverse relationship with effective strain values [18, 19].

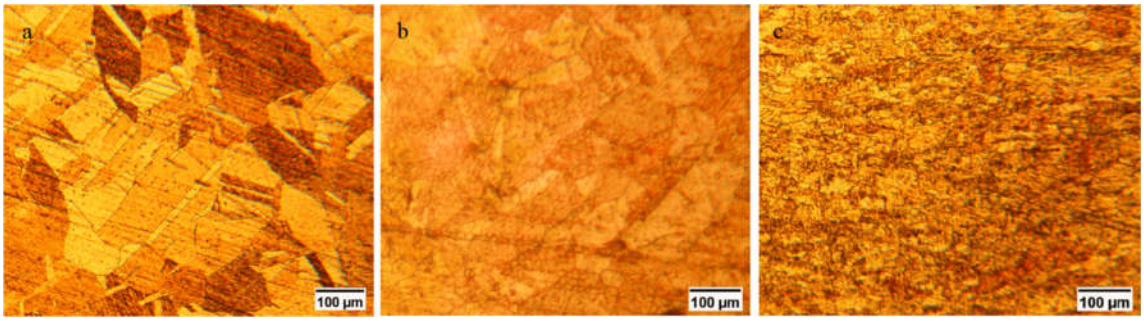

Figure 2. Optical micrographs of samples a) as-received, b) first pass and, c) final pass of CSP process

3.2 *XRD results*

Figure 3 shows the XRD patterns of the first and tenth passes of CSPed samples and the annealed sample. Compared to the annealed sample, the width of the peaks has increased with the increase of pass for the first and tenth passes. One of the reasons for the increase in the width of the peaks is strain in crystal lattice and grain refinement [20]. These phenomena are caused by intense strain [21]. Williamson--Hall equation was used to calculate the grain size. Next, with the help of the calculated grain size, the dislocation density was also investigated. The dislocation density (ρ) was calculated from equations (1)--(3) [22] as follows:

$$\rho = (\ [\![\rho\_D\ \rho\_\varepsilon)]\!]\ \hat{}0.5 \qquad (1)$$

$$\rho\_\varepsilon = k(\varepsilon\hat{}2)/b\hat{}2 \qquad (2)$$

$$\rho\_D = (3/D\hat{}2\ ) \qquad (3)$$

Where ρ_ε and ρ_D is dislocation due to lattice strain and domain size, respectively, k is material constant, D is size of grains, b is Burger's vector, and ε is lattice strain. Table 3 shows the grain size and density of dislocations

for the annealed and CSPed samples. According to Table 2, the grain size after the first pass has decreased from 27 μm to 11 μm, compared to the annealed sample. By increasing the applied strain in the 10th pass, the grain size decreases to 0.75 μm.

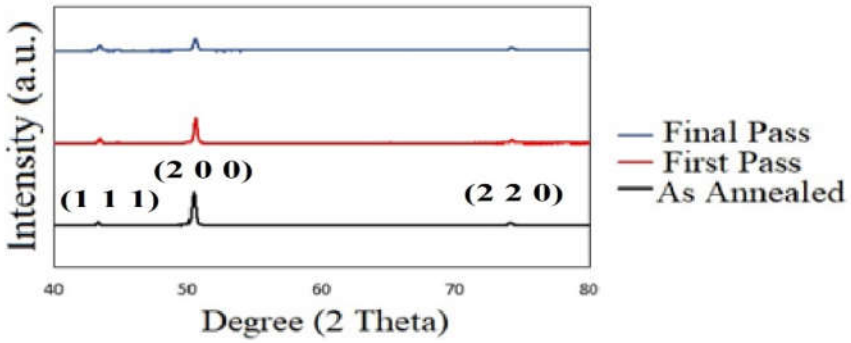

Figure 3. XRD patterns for a) the annealed sample, b) the first pass and b) the final pass produced by CSP

The density of dislocations for the as annealed, first and final passes are 1.004 (1/nm^2), 1.643 (1/nm^2), and 2.254 (1/nm^2), respectively. The results showed that by increasing the amount of applied strain in the final pass, it created the highest dislocation density in the microstructure. As a result, with the increase in the density of dislocations followed by dynamic recovery, it caused the largest decrease in grain size compared to other samples. However, the smallest reduction in grain size was obtained after applying one pass to the sample.

Table 2. Values of grain size and density of dislocations for the annealed sample, first and tenth passes of the CSP

Pass No.	Grain size (nm)	ρ (1/nm^2)
As annealed	27000	1.004
1	11000	1.643
10	750	2.254

3.3 *Residual stress analysis*

Residual stresses are equilibrium stresses that remain in the samples; therefore, it is very important to know amount and direction of Residual stresses. Plastic deformation leads to the creation of residual stresses. X-ray diffraction is one of the non-destructive methods to check the residual stress. Unlike the method of measuring grain size and dislocation density values, in the method of measuring residual stress with the Sin2ψ technique, the X-ray diffraction test is performed at a fixed angle of 2θ greater than 100 degrees (if any) and the d graph is drawn in terms of Sin2ψ. While in order to measure the density of dislocations and the size of crystals by XRD, the scanning range is 40-80 degrees. Principles and basics of residual stress are measured by the standard XRD method [23]. The most common method is Sin2ψ. Figure 4 shows X-ray diffraction patterns for three samples of annealed pure copper, CSPed samples of first and tenth passes. According to Figure 4, the tensile residual stress values decreased from +153.2 MPa in the annealed sample to +97.3 MPa in the first pass sample. In the tenth pass, the compressive residual stress was -48.6 MPa. With the increase of the effective plastic strain applied in higher passes, not only the strain distribution becomes uniform, but the residual stresses also change from tensile to compressive. Preventing the initiation and growth of cracks is the most important function of compressive residual stresses [24, 25].

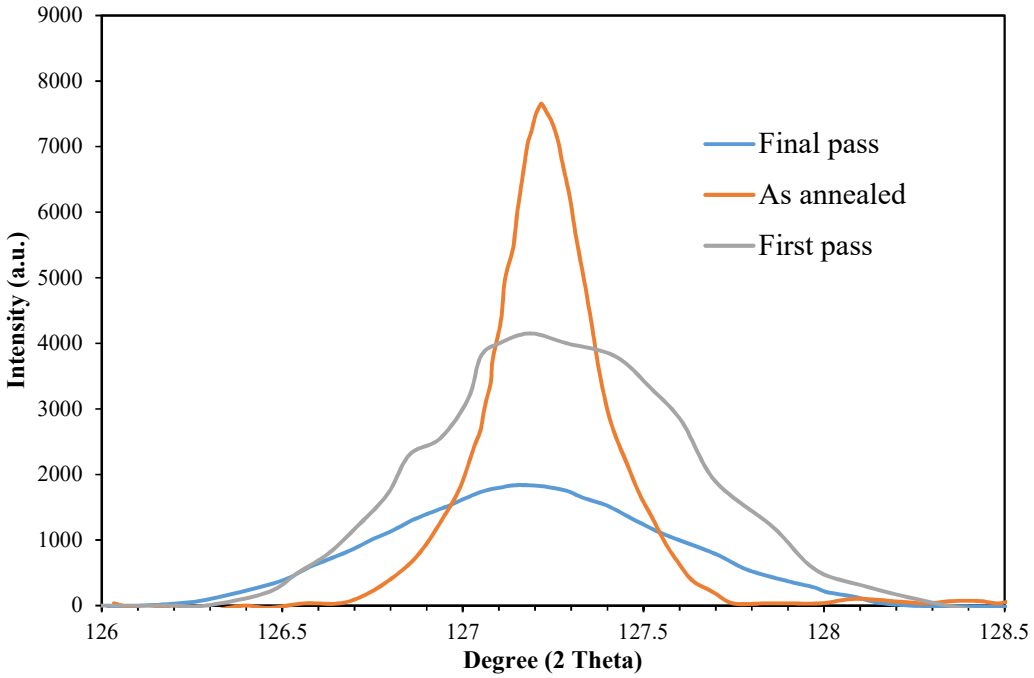

Figure 4. Residual stress for (a) as annealed, (b) first pass, and (c) tenth pass of CSPed sheets measured by XRD

3.4 *Residual stress analysis using simulation*

In this article, to simulate the software, DEFORM-3D is used. According to the geometry of the die, the simulation of the method was performed in three dimensions. The dies are considered rigid. In addition, the volume control feature was considered during the simulation. The friction between the plate and dies is considered to be of Columbus type with a coefficient of 0.1 and the speed of the upper die is 0.1 mms^{-1}. The behavior of the copper sheet is considered elastic-plastic. For copper sheet, to describe the plastic deformation behavior, the material model was selected using the Johnson-Cook equation of state according to equation (4) as follows:

$$\sigma = (A + B\,\varepsilon^{n})\left(1 + C\ln\left(\frac{\dot{\varepsilon}}{\dot{\varepsilon}_0}\right)\right)\left[1 - \left(\frac{T - T_r}{T_m - T_r}\right)^{m}\right] \quad (4)$$

Here A, B, m, n, and c are constants and are chosen for each material according to its properties. Also, $\dot{\varepsilon}, \dot{\varepsilon}_0, T, T_m, T_r$ are strain, the reference plastic strain rate, temperature, melting temperature and room temperature, respectively. Johnson-Cook constants, physical and mechanical properties of copper sheets are shown in Tables 3 and 4, respectively.

Table 3. Johnson--Cook equation of state coefficients for pure copper

***A* (MPa)**	***B* (MPa)**	***c***	***n***	***m***	**T melt (°C)**
90	292	0.025	0.31	1.09	25

Table 4. Elastic properties and density of copper

density (kg/m^3)	**Young's modulus (MPa)**	**Poisson's ratio**
93.8	125000	0.34

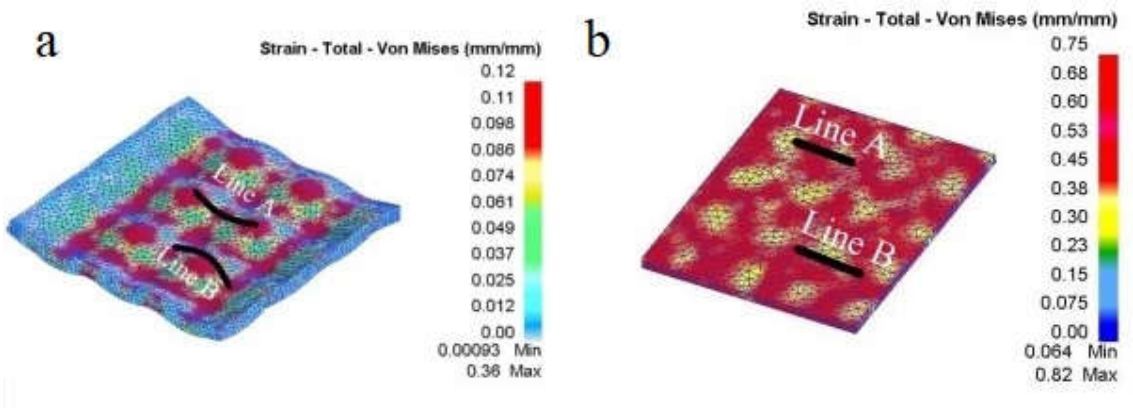

Figure 5. Schematic representation of the directions of residual stress distribution of a) corrugation step, b) straightening step (line A in the valley and line B on the peaks)

Figure 5 shows the distribution of the residual stress for the first pass of the CSPed sheet in the numerical simulation with DEFORM-3D software. Figure 5 displays lines A and B as the direction for considering the residual stress distribution σX in valley and peak, respectively. Figure 6 displays the distribution of residual stress σX in the first step of corrugation. According to Figure 6-a, the residual stress values in the corrugation step in the valleys are tensile. After that according Figure 6-b, in the same direction as the straightening step, not only the values of tensile stresses have decreased, but also compressive stresses are observed. In this regard, the residual stress distribution includes a range between +8 and 4 MPa. As shown in Figure 7-a, the residual stress values are distributed along line B in the form of tension and compression in the corrugation step, whereas in Figure 7-b, almost the residual stresses change to compressive values. In this regard, the residual stress distribution includes a range between +1 and 6 MPa. According to Figures 4, 5,6, and 7, based on residual stress analysis using the Sin2ψ method and simulation, tensile stress values are redistributed to compressive stress for the straightening step. Therefore, by applying more strains in the CSP technique, the values of compressive stresses increase, which is a factor to prevent the growth of cracks.

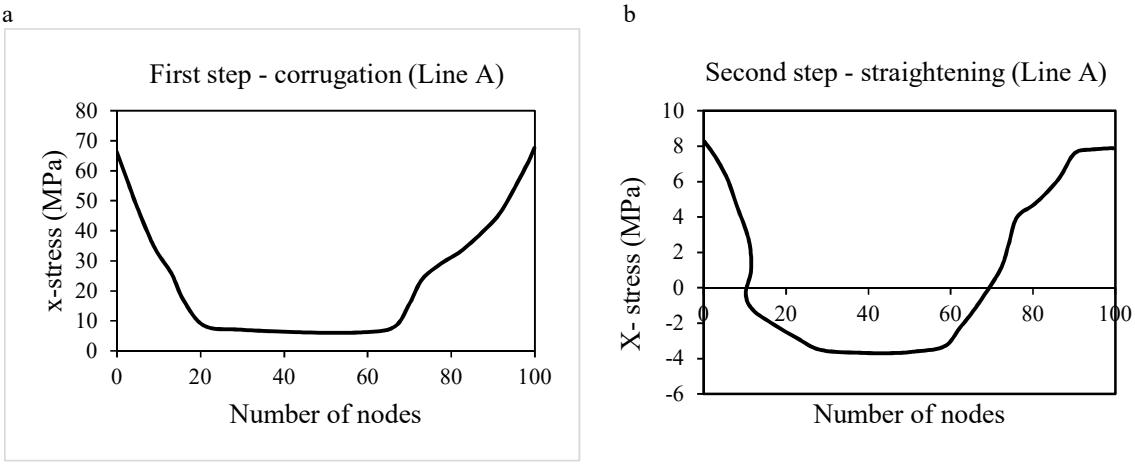

Figure 6. Distribution of residual stress σ_X on path A a) corrugation step and b) straightening step in the first pass

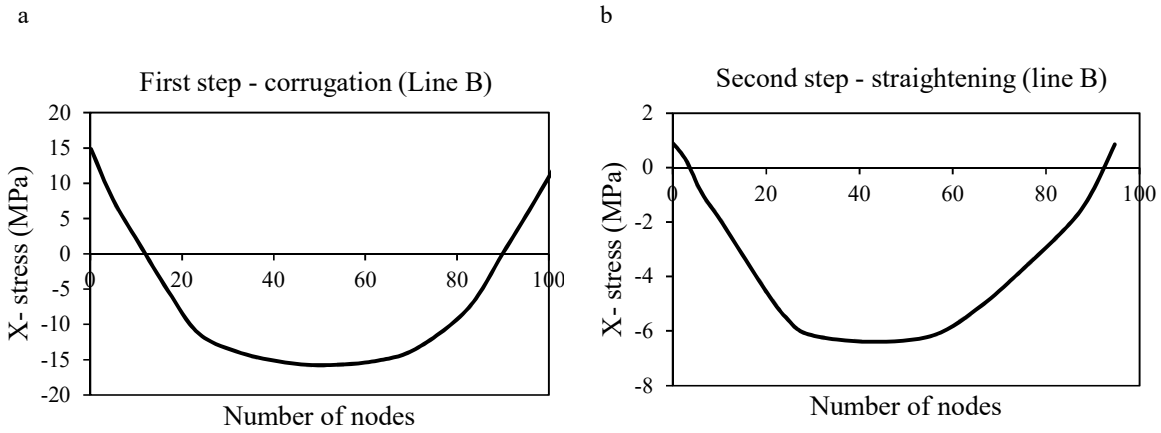

Figure 7. Distribution of residual stress σ_X on direction B a) corrugation step and b) straightening step in the first pass

4. Conclusion

This study investigated the microstructural evaluation and residual stresses of copper sheets produced by CSP. First, the simulation for the first pass of CSP technique on pure copper sheets was investigated. The distribution of residual stresses and effective plastic strain were studied by simulation. In addition, the microstructural properties of annealed copper sheet samples, first pass and tenth pass were investigated. In addition, using the X-ray diffraction method, changes in grain size, density of dislocation and residual stress of copper samples were investigated. The results are as follows:

a) The FEM simulation results designate that the amount of equivalent plastic strain is 0.82 for the first pass in the CSP process.

b) The average grain size is 27 μm for the annealed sample while the average grain size decreased to 11 μm for the first pass. After 10 passes, the average grain size was reduced to 750 nm.

c) The density of dislocations for the as annealed, first and final passes are 1.004 ($1/nm^2$), 1.643 ($1/nm^2$), and 2.254 ($1/nm^2$), respectively.

d) With increasing number of passes, the dislocation density increases considerably, while the grain size decreases significantly.

e) The residual stresses were altered from +153.2 MPa for the annealed sample to -48.6 MPa in the 10th pass sample.

f) By increasing the number of passes, the sign of the residual stress has changed from tensile to compressive, which is the cause of the delay in crack growth.

g) Consistent with the results of numerical simulation, the initiation and growth of cracks is delayed, by reason of the alteration in the sign of residual stress from tensile to compressive.

h) The width of the peaks has increased with the increase in the amount of strain for tenth passes, which indicates the grain refinement.

Conflicts of Interest

The author declares no conflict of interest associated with this manuscript.

References

1. Torabzadeh KH, Kashi H, Faraji G. A review of the production of ultrafine grained and nanograined metals by applying severe plastic deformation. *Modares Mech. Eng.*, 2016, 16:271-282.
2. Zhu YT, Honggang J, Huang J, Lowe TC. A new route to bulk nanostructured metals. *Metall. Mater. Trans.*, 2001, 32:1559-1562.
3. Shin DH, Park JJ, Kim YS, Park KT. Constrained groove pressing and its application to grain refinement of aluminum. *Mater. Sci. Eng. A*., 2002, 328:98-103.
4. Torkestani A, Dashtbayazi MR. A new method for severe plastic deformation of the copper sheets. *Mater. Sci. Eng. A*., 2018, 737:236-244.
5. Kaykha MM, Dashtbayazi MR. Experimental and numerical investigation of severe plastic deformation of copper sheets processed by modified-constrained studded pressing. *Mater. Res. Express.,* 2022, 9(1):016523.
6. Thangapandian N, Prabu SB. The role of corrugation die parameters on the mechanical properties of aluminum alloy (AA 5083) processed by repetitive corrugation and straightening. *J. Chem. Eng. Mater. Sci.*, 2015, 3(7):208-212.
7. Lee JW, Park JJ. Numerical and experimental investigations of constrained groove pressing and rolling for grain refinement. *J. Mater. Process. Technol.,* 2002, 130:208-213.
8. Yoon SC, Krishnaiah A, Chakkingal U, Kim HS. Severe plastic deformation and strain localization in groove pressing. *Comput. Mater. Sci.,* 2008, 43(4):641-645.
9. Wang ZS, Guan YJ, Song LB, Liang P. Finite element analysis and deformation homogeneity optimization of constrained groove pressing. *Appl. Mech. Mater.,* 2013, 278:505-513.
10. Kumar S, Hariharan K, Digavalli R. Hybrid optimization of die design in constrained groove pressing. *J. Manuf. Process.,* 2020, 35(6):687-699.
11. Sajadi A, Ebrahimi M, Djavanroodi F. Experimental and numerical investigation of Al properties fabricated by CGP process. *Mater. Sci. Eng. A.,* 2012, 552:97-103.
12. Thangapandian N, Prabu SB, Padmanabhan KA. On the role of experimental variables in the repetitive corrugation and straightening of an Al-Mg alloy. *Procedia Eng.,* 2017, 207:1457-1462.
13. Elizalde S, Ezequiel M, Figueroa IA, Cabrera JM, Braham C, Gonzalez G. Microstructural evolution and mechanical behavior of an Al-6061 alloy processed by repetitive corrugation and straightening. *Metals,* 2020, 10(4):489.
14. Shahraki S, Miyanaji H, Abdollahi H. Microstructure and mechanical properties of ultrafine-grained IF steel sheets produced by constrained groove pressing. *Eng. Solid Mech.,* 2020, 8(1):63-68.
15. Nazari F, Honarpisheh M. Analytical and experimental investigation of deformation in constrained groove pressing process. *Proc. Inst. Mech. Eng. C J. Mech. Eng. Sci.,* 2019, 233(11):3751-3759.
16. Jefferies Z, Kline AH, Zimmer EB. The determination of grain size in metals. *Trans. AIME,* 1916, 57:594-607.
17. Mote VD, Purushotham Y, Dole BN. Williamson-Hall analysis in estimation of lattice strain in nanometer-sized ZnO particles. *J. Theor. Appl. Phys.,* 2012, 6:1-8.
18. Lowe TC, Valiev RZ. The use of severe plastic deformation techniques in grain refinement. *Jom*, 2004, 56:64-68.

19. Gupta AK, Maddukuri TS, Singh SK. Constrained groove pressing for sheet metal processing. *Prog. Mater. Sci.*, 2016, 84:403-462.
20. Cullity BD. Elements of X-ray Diffraction. Boston: Addison-Wesley Publishing, 1956.
21. Adachi T, Sekino T, Nakayama T, Kusunose T, Niihara K. Measurement of microscopic stress distribution of multilayered composite by X-ray stress analysis. *Mater. Lett.,* 2003, 57(20):3057-3062.
22. Khayati GR, Janghorban K. Thermodynamic approach to synthesis of silver nanocrystalline by mechanical milling silver oxide. *Trans. Nonferrous Met. Soc. China,* 2013, 23(2):543-547.
23. Auld JH, Greenough GB. Residual lattice strains in iron single crystals. *Acta Metall.*, 1954, 2(2):209-213.
24. Totten GE. Handbook of residual stress and deformation of steel. Ohaio: ASM International, 2002.
25. Rossini NS, Dassisti M, Benyounis KY, Olabi AG. Methods of measuring residual stresses in components. *Mater. Des.,* 2012, 35:572-588.

How to cite this article: Kaykha MM. Effect of Constrained Studded Pressing on the Microstructure and Residual Stresses for Producing Nanostructure Pure Copper Sheet. *Curr. Appl. Sci.*, 2025, 3(1):47-56. https://doi.org/10.22034/cas.2024.456324.1039